



An Analysis of OFDM Peak Power Reduction Techniques for WiMAX Systems

Cristina Ciochina^{(1),(2)}, Fabien Buda⁽¹⁾ and Hikmet Sari^{(1),(2)}

⁽¹⁾ Sequans Communications, 19 Le Parvis, 92073 Paris La Défense, France

⁽²⁾ Supélec, 1-3 Rue Joliot Curie, 91190 Gif sur Yvette, France

Abstract – The main drawback of Orthogonal Frequency Division Multiplexing (OFDM) systems is the high peak-to-average power ratio (PAPR), which significantly reduces the efficiency of the transmit high power amplifier (HPA). Several methods have been proposed in the literature to reduce the peak power of OFDM signals and substantial gains were reported. In this paper, the effectiveness of some recently proposed methods is evaluated for WiMAX systems. Using typical HPA models and spectral masks, these PAPR reduction methods are evaluated in terms of the total system degradation.

I. INTRODUCTION

Although the first applications of multicarrier systems date back to the late 1950's, it is only recently that this transmission technique has found acceptance as a valid alternative to single-carrier systems. Coded orthogonal frequency-division multiplexing (OFDM) schemes are today used for terrestrial digital video broadcasting (DVB-T), digital audio broadcasting (DAB-T), wireless local area networks (IEEE 802.11a, ETSI Hiperlan2) and wireless metropolitan area networks (IEEE 802.16d).

The well-known advantages of OFDM that have made this technique popular in wireless systems are sometimes counter-balanced by one major problem: The high peak-to-average power ratio (PAPR) of this signal format significantly reduces the average power at the output of the high-power amplifier (HPA) used at the transmitter. Indeed, the input signal must lie in the linear region of the HPA, which is well below the saturation power and the increased linear dynamic range requirements impose the use of very expensive HPAs.

In order to avoid the extremely high back-offs and costly amplifiers, occasional clipping and/or soft thresholding must be allowed. This phenomenon leads to in-band distortion that increases the bit error rate (BER) and to spectral widening that increases adjacent channel interference.

A large number of methods have been developed in order to reduce the peak power of OFDM signals. Among these, the Active Constellation Extension (ACE) in its POCS (Projection onto Convex Sets) variant is a rather simple and elegant method which was reported to give promising results for use in commercial systems [1]. In this paper, we analyze the performance of this method and compare the theoretical gains promised in the literature with those achieved in a real-world situation. The focus in this study is on WiMax systems based on the OFDM mode of the IEEE 802.16d specifications. The performance evaluation is conducted in terms of PAPR reduction, energy distribution, back-off reduction, power spectral density after the HPA, and BER at the receiver. The study takes into account practical system constraints such as the HPA type and power radiation masks to be respected.

This paper is organized as follows: In section II, the PAPR problem in OFDM is formulated. Section III reviews the conventional PAPR reduction techniques with a strong focus on the ACE-POCS method. Performance evaluation criteria

are presented and the results are discussed in section IV. Finally, the conclusions are given in section V.

II. PAPR PROBLEM IN OFDM

An OFDM signal is the sum of N independent QAM symbols mapped onto N different subchannels with $1/T$ frequency separation where T is the OFDM symbol period. The discrete time-domain samples $\mathbf{b}^i = (b_0^i, b_1^i, \dots, b_{N-1}^i)$ to be transmitted are obtained via an N -point inverse Fast Fourier Transform (IFFT) from the complex QAM symbols block $\mathbf{a}^i = (a_0^i, a_1^i, \dots, a_{N-1}^i)$:

$$b_n^i = \frac{1}{\sqrt{N}} \sum_{m=0}^{N-1} a_m^i e^{j2\pi mn/N}, \quad (1)$$

where a_m^i is the QAM data symbol sent on the m th subcarrier of the i th OFDM symbol. The OFDM symbol index will be omitted in the sequel.

A cyclic prefix is usually appended. Prior to passing through the HPA, the OFDM signal goes through D/A conversion, eventually analog filtering, and it is mapped on a carrier frequency.

For large N , the time domain samples b_m^i have a zero-mean Gaussian-like distribution, as they are weighted sums of independent identically distributed random variables (the frequency-domain QAM symbols a_n^i). A small percentage of these time-domain samples are therefore susceptible to having high magnitudes (the tail of the distribution). These high magnitude samples cause the PAPR problem in OFDM.

Mathematically, the PAPR of an OFDM block of digital samples $\mathbf{b} = (b_0, b_1, \dots, b_{N-1})$ is defined as:

$$PAPR(\mathbf{b}) = \frac{\max_{0 \leq n \leq N-1} |b_n|^2}{E\{\|\mathbf{b}\|^2\}/N}, \quad (2)$$

where $\|\cdot\|$ denotes the Euclidean norm of the enclosed vector. An analog equivalent can also be defined, and in practice it is the PAPR of the continuous-time signal that is of interest (oversampling and D/A conversion lead to peak regrowth). It can be proven [4] that the digital PAPR of the OFDM signal oversampled at a rate of $L=4$ gives a good approximation of the equivalent continuous-time PAPR.

It should also be noted that the baseband PAPR as defined above is 3dB lower than the corresponding passband PAPR.

III. CONVENTIONAL PAPR REDUCTION METHODS

A large number of OFDM PAPR reduction techniques have appeared in the literature during the past decade, all having the purpose of reducing the required HPA back-off and the effects of its nonlinearity. The various approaches are quite different from each other and impose different constraints.

First, coding [5] relies on using several bits or bit sequences which would carry a properly chosen code (sometimes with error correcting capabilities) that minimizes the PAPR of the resulting transmitted signal. The PAPR is reduced, but so is the data rate. Other methods use phase manipulations (e.g. Selective Mapping – SLM, Partial Transmit Sequences – PTS, Random Phasor) [6-8]. Although very effective, these methods have a high complexity and also require coded side information to be transmitted. This fact raises problems in terms of compliance to standards.

Other methods such as Tone Reservation [4] propose inserting anti-peak signals in unused or reserved subcarriers. The method does not cause any in-band distortion, but it reduces the useful data rate. Although suited in some implementations (IEEE 802.16e for example), it is not always standard compliant (the bandwidth sacrifice required by this method is not acceptable in IEEE 802.16d).

Another family of methods proposes altering the QAM constellation in order to reduce high signal peaks. The first method relying on the principle of constellation expansion was Tone Injection [4]. It involves a complex optimization process that makes it scarcely attractive for systems with a high number of carriers.

Simpler constellation extension methods were recently developed. Active constellation extension (ACE) [1] allows the corner QAM constellation points to be moved within the quarter planes outside their nominal values. The other border points are allowed to be displaced along rays pointing towards the exterior of the constellation. The interior points are not modified, in order to preserve the minimum distance between the constellation symbols. Such a constellation modification is represented in Fig. 1 for the 16QAM constellation. Suboptimal versions of the ACE algorithm (POCS, AGP, SGP) are also described in literature.

More recently, a simple non-iterative PAPR reduction method relying on metric-based symbol predistortion (MBSP) was proposed in [3]. A predetermined number of corner constellation symbols (and the real or the imaginary part of symbols on the sides of the constellation) are multiplied with a real-valued constant greater than unity. A cost function that

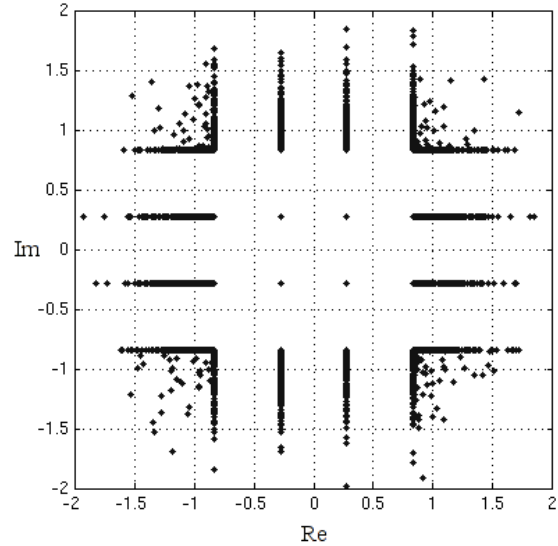


Figure 1. ACE constellation shaping for 16QAM signal mapping.

involves the magnitudes $|b_n|$ and the angles between the b_n samples and the contribution of the a_m symbol to those samples determines which symbols are to be modified. This algorithm is not recursive and it does not require the transmission of any side information. The number of symbols to be modified and the real-values expansion factor are predetermined by means of simulation.

From all of the algorithms described above, only the last two are suited for a practical implementation in a system compliant to the IEEE 802.16d standard.

IV. SIMULATION RESULTS

A. System Model

In this paper, the simulated system employs an OFDM signal with $N = 256$ subcarriers, among which 192 data carriers (QPSK, 16QAM or 64QAM signal mapping), 8 pilots (BPSK modulation), 1 DC and 56 guard carriers (28 lower and 27 upper frequency guard subcarriers). For simplicity, uncoded OFDM will be employed.

The HPA is Rapp's solid state power amplifier model (SSPA) [10] with the characteristic

$$v_{OUT} = \frac{v_{IN}}{\left(1 + (|v_{IN}|/v_{SAT})^{2p}\right)^{\frac{1}{2p}}}, \quad (3)$$

where v_{IN} , v_{OUT} are respectively the complex input and complex output signals (baseband equivalent, normalized) and v_{SAT} corresponds to the output saturation level, $P_{SAT} = |v_{SAT}|^2$, normalized to unity. The parameter p , often called "knee factor," controls the smoothness of the characteristic (the smaller p the smoother the characteristic).

Throughout this paper, we consider a Rapp model HPA with knee factor $p = 2$, since it is indicated [9] to be a good representation of typical power amplifiers in the sub-10GHz frequency range. The results will be compared with those obtained in the ideal case of a clipper amplifier.

We also define the input back-off (IBO) and output back-off (OBO) with respect to the saturation values:

$$IBO|_{dB} = -10 \log_{10} \frac{E\{|v_{IN}(t)|^2\}}{P_{SAT,IN}}, \quad (4)$$

$$OBO|_{dB} = -10 \log_{10} \frac{E\{|v_{OUT}(t)|^2\}}{P_{SAT,OUT}}. \quad (5)$$

B. ACE-POCS Algorithm

When applying the ACE-POCS algorithm described in [1] we must take into account some system constraints: Neither the pilots nor the guard intervals are allowed to be modified. The ACE-POCS method can be described as follows:

- Given the input block \mathbf{a} consisting of 256 samples (data, guard and pilots), we compute via IFFT the output sequence \mathbf{b} .
- All peaks corresponding to $|b_n| > A$, where A is a certain threshold, are clipped in magnitude in order to obtain:

$$\tilde{b}_n = \begin{cases} b_n, & \text{if } |b_n| \leq A \\ Ae^{j\theta_n}, & \text{otherwise} \end{cases}, \quad (6)$$

where $b_n = |b_n|e^{j\theta_n}$, $n = 1 \dots 256$.

- Compute $\tilde{\mathbf{a}} = FFT(\tilde{\mathbf{b}})$.
- Apply the constraints, i.e., restore the initial values for the pilots and guards and project the constellation points into the region of increased margin (as in Fig. 1).
- Return to the first step and iterate until no peaks are clipped, the PAPR is essentially minimized or a certain number of iterations is reached.

Several different versions of this algorithm can be devised in order to reduce the number of iterations (mainly gradient based methods). Nevertheless, gradient based methods are more appropriate when the goal is to minimize the value of the highest peak rather than to achieve a fixed maximum peak level, as necessary in our case.

In the following, the ACE-POCS algorithm is applied for a threshold A set at 3.35 dB above the average signal power and 10 iterations were carried out. An oversampling with rate $L = 4$ is performed after having applied the PAPR algorithm (before passing through the HPA).

C. Several Performance Criteria

The purpose of PAPR reduction techniques is to alleviate the back-off requirements and/or to reduce the effects of HPA nonlinearity. From a practical standpoint, back-off reduction is therefore an important parameter for evaluating the effectiveness of a given PAPR reduction technique.

In the literature, it is customary to use the Complementary Cumulative Distribution Function (CCDF) of the PAPR as a performance criterion. The CCDF of the PAPR is defined as the probability that the PAPR per OFDM symbol exceeds a certain clipping level γ^2 .

$$CCDF(PAPR(\mathbf{b})) = \Pr(PAPR(\mathbf{b}) > \gamma^2). \quad (7)$$

Fig. 2 presents the CCDF of PAPR for the ACE-POCS algorithm in the conditions described above. The solid-line curve corresponds to the conventional OFDM signal and the marked lines correspond to the signal after 10 ACE-POCS iterations. The average power increase is of 0.78 dB, 0.39 dB and 0.2 dB for the QPSK, 16QAM and 64QAM respectively. Oversampling was performed after applying the PAPR reduction algorithm. Simulations were also performed in the case when the algorithm is applied to the oversampled OFDM signal. The results are slightly better, but the small additional gain (on the order of 0.3 dB) does not justify the complexity increase (the FFT length is multiplied by L).

Suppose that the system constraints (spectrum masks, BER requirements) impose a 9 dB IBO and that we use QPSK signal mapping. In the case of an ideal clipper amplifier, the CCDF of PAPR can be interpreted directly. The OFDM symbols distorted when passing through the amplifier are only those with a PAPR higher than 9 dB. Clipping of the original signal occurs with a probability of $3 \cdot 10^{-4}$. After applying the ACE-POCS algorithm, an IBO of only 6.7 dB is necessary in order to preserve the same clipping probability. The 2.3 dB gain in IBO is achieved at the expense of a 0.55 dB loss in E_b/N_0 (at a target BER of 10^{-5}), due to average power increase that is inherent to the ACE-POCS algorithm. The spectrum shown in Fig. 3 confirms this interpretation.

In the case of a Rapp model amplifier with $p = 2$ (a case often encountered in practice), the distortion is due to all samples falling in the nonlinear zone of the HPA input-output characteristic, not only to those that fall in the saturation region. The spectrum analysis presented in Fig. 4 shows that

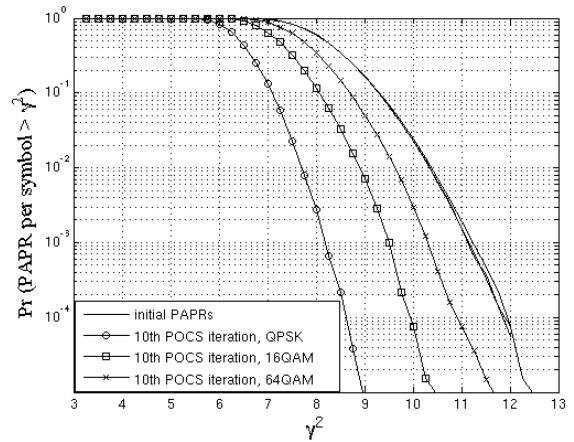


Figure 2. CCDF of PAPR results for the ACE-POCS method applied to the OFDM system with QPSK, 16QAM and 64QAM signal mapping, followed by oversampling to $L = 4$.

the gain to be expected in practice is much smaller than that predicted by the CCDF of PAPR curves: Only 1dB of gain in the favorable case, where a 9 dB IBO would be necessary. The OBO is reduced from 9.17 dB to 8.18 dB for the same spectral shape and the additional E_b/N_0 loss is 0.6 dB.

In practice, the back-off required to comply with typical spectrum masks can be significantly lower than the 9 dB value considered above. Typical back-off values allowing such a system to comply with ETSI masks type E/F/G [11] (corresponding to QPSK, 16QAM and 64QAM, respectively) with an acceptable BER degradation are on the order 5-7 dB. In this case, the probability that at least one sample per OFDM symbol goes into saturation is very high, and the CCDF of PAPR curves are no longer interpretable.

Moreover, the CCDF of PAPR is a representation that takes into account only one sample per OFDM signal (the highest peak). From a practical point of view, we are not interested only in the sample with the largest magnitude, but in all the $|b_n|$ samples that are in the nonlinear zone and/or go into saturation, as they all produce distortion. It is therefore more interesting to analyze the CCDF of the instantaneous normalized signal power (INP) defined as:

$$\text{CCDF}(\text{INP}(v_{IN})) = \Pr\left(\frac{|b_i|^2}{P_{\text{avg},IN}} > \gamma^2\right) \quad (8)$$

where v_{IN} is the signal present at the input of the HPA (after PAPR reduction), $P_{\text{avg},IN} = E\{|v_{IN}(t)|^2\}$ is its average power.

The CCDF of INP in Fig. 5 gives a good approximation of the maximum gain that can be obtained in the ideal case of using a clipper-type HPA, at a certain clipping probability or when working at a certain IBO. The solid-line curves correspond to the conventional OFDM signal and the marked lines correspond to the signal after 10 ACE-POCS iterations in the case of different signal mappings. Oversampling to $L = 4$ was performed after having applied the PAPR reduction algorithm. When using an ideal clipper model HPA, the curves can be directly read and they give a more reliable estimation than those in Fig. 2.

Let us now consider the case where the system uses QPSK signal mapping and it must comply with the ETSI EN301.021 v1.6.1 mask type E. The HPA was modeled as a Rapp amplifier $p = 2$. The mask type and the amplifier type impose the necessary back-off, since in this case the spectral constraints are more restrictive than the BER requirements. The necessary IBO when no PAPR reduction is performed is of 4.4 dB (equivalent OBO of 5.28 dB, see Fig. 6). As the CCDF of INP predicts, the gain will be rather small at this back-off value. When applying the ACE-POCS algorithm, the necessary back-off in order to comply with the spectral constraints is only reduced by 0.7 dB. This rather small gain is obtained at the expense of an increase of the computational complexity and also of the transmit power that is inherent to the PAPR reduction method. In this case, no significant gain

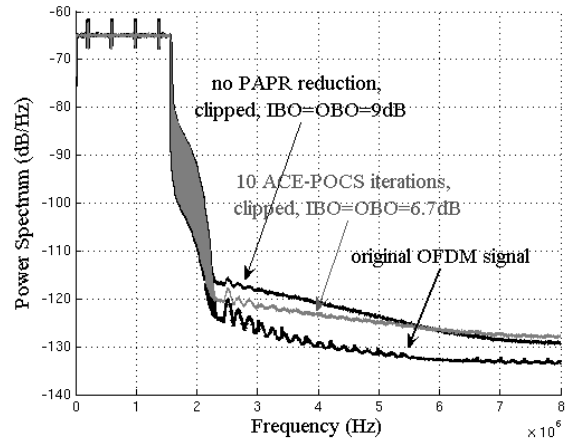


Figure 3. Spectrum of an OFDM QPSK signal, with and without ACE-POCS treatment, $L=4$ oversampling, clipper-type ideal HPA.

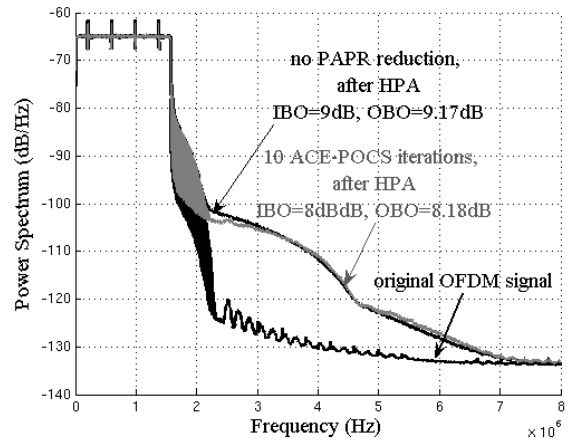


Figure 4. Spectrum of an OFDM QPSK signal with and without ACE-POCS processing, $L=4$ oversampling, HPA Rapp $p=2$.

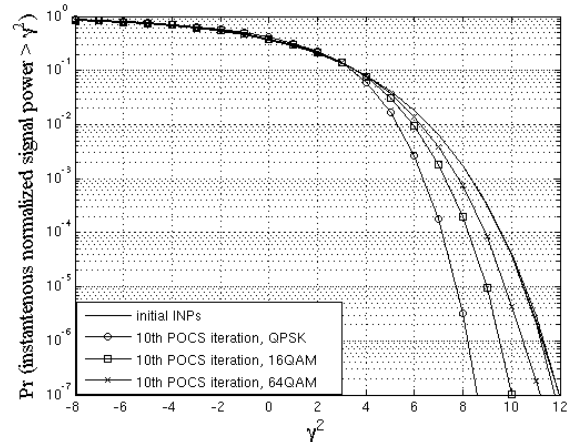


Figure 5. CCDF of instantaneous normalized signal power (INP) results for the ACE-POCS method applied to the OFDM system with QPSK, 16QAM and 64QAM signal mapping, followed by oversampling to $L = 4$.

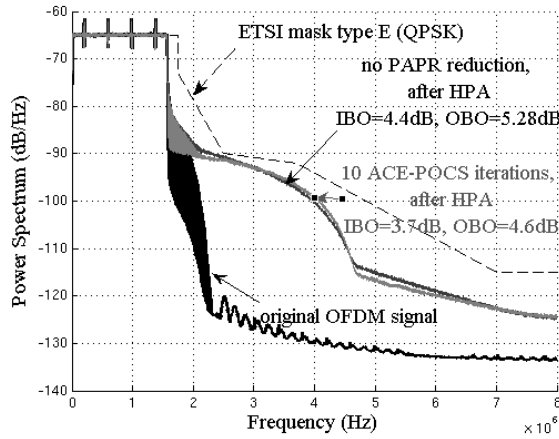


Figure 6. Spectrum of an OFDM QPSK signal, with and without ACE-POCS processing, complying with ETSI mask type E, HPA Rapp $p=2$.

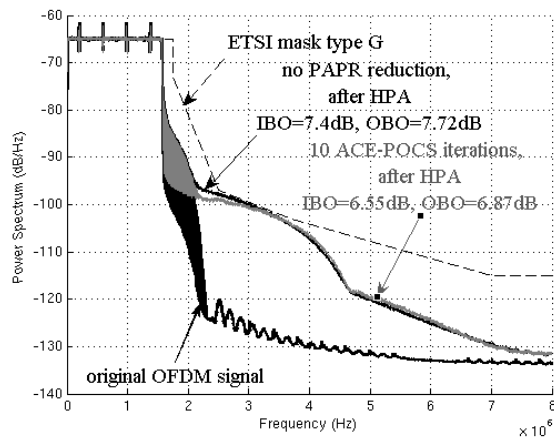


Figure 7. Spectrum of an OFDM QPSK signal, with and without ACE-POCS processing, complying with ETSI mask type G, HPA Rapp $p=2$.

is obtained that truly justifies the use of the PAPR reduction method.

Even for QPSK signal mapping, a higher input back-off might be required in practice. For example, if adaptive modulation schemes are used, the system is required to comply with the most restrictive spectral mask, which is the ETSI mask type G for 64 QAM (see Fig. 7).

The necessary back-off can be reduced by approximately 0.9 dB (the maximum gain in the case of an ideal nonlinearity is 1.6 dB as indicated in Fig. 5). Using higher-order modulations would obviously lead to even smaller gains: at most 0.8 dB in the case of 16QAM modulation and 0.4 dB in the case of 64QAM.

In order to approximate the real attainable gains, an estimation of the total degradation ($E_b/N_0 + OBO$ loss when compared to the ideal case of an OFDM signal in the absence of the nonlinearity) was also performed.

Fig. 8 and Fig. 9 show the total degradation at the BER targets of 10^{-4} and 10^{-5} . As stated above, these simulations

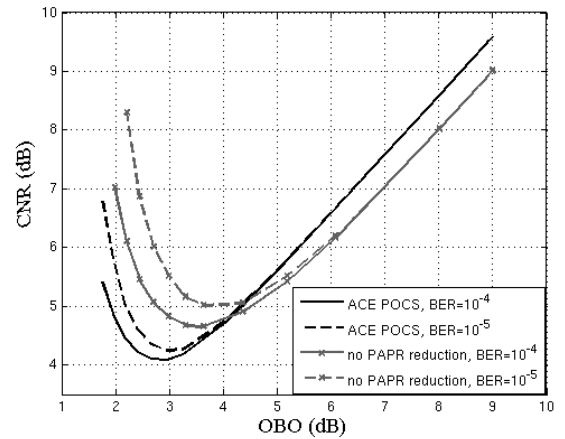


Figure 8. Total degradation versus OBO, OFDM QPSK signal, with and without ACE-POCS processing, clipper-type ideal HPA.

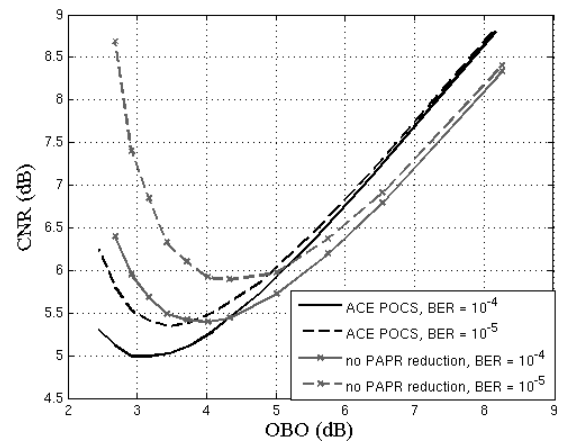


Figure 9. Total degradation versus OBO, OFDM QPSK signal, with and without ACE-POCS processing, HPA Rapp $p=2$.

correspond to the uncoded OFDM case. The gray curves correspond to the OFDM signal without any PAPR reduction processing passed through a clipper amplifier and a Rapp HPA with knee factor $p = 2$, respectively. The black curves depict the behavior of the system when 10 ACE POCS iterations are performed.

Analyzing the curves in Fig. 9, we can deduce that when no PAPR reduction is performed, the simple fact of passing through the HPA Rapp $p = 2$ causes a loss of at least 5.4 dB (at the BER of 10^{-5}). Applying the algorithm allows us to reduce the minimum total degradation to 5 dB. At small back-off values, the degradation is due to the important in-band distortion, which imposes the necessity of increasing E_b/N_0 in order to preserve the BER. When the back-off increases, the degradation caused by the nonlinearity is smaller, and the PAPR reduction algorithm produces a supplementary degradation due to the constellation modification: A higher transmitted power is necessary in order to preserve the minimum constellation distance and the BER target.

Reiterating the example in Fig. 7, we can determine the real gain obtained in this case. We have established that the system's working point is imposed by the spectral constraints and that the PAPR reduction algorithm allows us to reduce the OBO from 7.72 dB to 6.87 dB. If we contrast these values with the information in Fig. 9, we find that the total degradation is reduced from 7.92 dB to 7.6 dB, leaving an overall gain of 0.3 dB only.

IV. CONCLUSIONS

We have evaluated the effectiveness of constellation extension methods in a real system, taking as example the well-known ACE POCS method and using it in an IEEE 802.16d-type system, at a sufficient oversampling rate, with the most usual HPA models and spectral masks. The working point (back-off) of the system is imposed by the power radiation masks and the nonlinearity type, with the restriction of meeting the BER requirements. Since the required back-off values are rather small in this type of system, we proposed to use the CCDF of INP as a more relevant performance criterion than the widely used CCDF of PAPR. This gives a more detailed representation of the signal, since it takes into account all the signal samples susceptible of generating degradation when passing through the HPA, and not only the highest peak of the OFDM symbol.

Using typically employed HPAs, the results have shown that the gains achieved by this type of PAPR reduction method are significantly smaller than those predicted by the CCDF of PAPR curves. A similar analysis performed for the MBSP algorithm described in [3] has shown comparable

performance. In order to obtain the large gains promised by the CCDF of PAPR, not only high HPA back-offs, but also linearization methods are necessary.

REFERENCES

- [1] B. S. Krongold and D. L. Jones, "PAR Reduction in OFDM via Active Constellation Extension," *IEEE Transactions on Broadcasting*, vol. 3, pp. 258-268, September 2003.
- [2] H. K. Kwok and D. L. Jones, "PAR Reduction via Constellation Shaping," in *Proceedings of ISIT 2000*, Sorrento, Italy, June 2000.
- [3] S. Sezginer and H. Sari, "Peak Power Reduction in OFDM Systems Using Dynamic Constellation Shaping," *Proceedings of EUSIPCO 2005*, Antalya, Turkey.
- [4] J. Tellado, *Multicarrier Modulation with Low Peak to Average Power Applications to xDSL and Broadband Wireless*, Boston/Dordrecht/London: Kluwer Academic Publishers, 2000.
- [5] K. Patterson, "Generalized Reed-Muller Codes and Power Control in OFDM Modulation," *IEEE Transactions on Information Theory*, vol. 46, pp. 104-120, January 2000.
- [6] C. Tellambura, "Phase Optimization Criterion for Reducing Peak-to-Average Power Ratio in OFDM," *Electronics Letters*, vol. 34, pp. 169-170, January 1998.
- [7] M. Breiling, S. H. Muller, and J. B. Huber, "SLM Peak-Power Reduction without Explicit Side Information," *IEEE Communications Letters*, vol. 5, pp. 239-241, June 2001.
- [8] S. H. Muller and J. B. Huber, "OFDM with Reduced Peak-to-Average Power Ratio by Optimum Combination of Partial Transmit Sequences," *Electronics Letters*, vol. 33, pp. 368-369, February 1997.
- [9] T. Kaitz, "Channel and interference model for 802.16b Physical Layer," contribution to the IEEE 802.16b standard, 2001.
- [10] C. Rapp, "Effects of the HPA-nonlinearity on a 4-DPSK/OFDM signal for a digital sound broadcasting system," *Tech. Conf. ECSC'91*, Luettich, October 1991.
- [11] ETSI EN 301.021 v1.6.1, *Fixed Radio Systems; Point-to-multipoint equipment; TDMA; Point-to-multipoint digital radio systems in frequency bands in the range 3GHz to 11GHz*, July 2003.